

Phase Retrieval And Cryo-Electron Microscopy

<http://bicmr.pku.edu.cn/~wenzw/bigdata2017.html>

Acknowledgement: this slides is based on Prof. Emmanuel Candès 's and Prof. Amit Singer's lecture notes

Outline

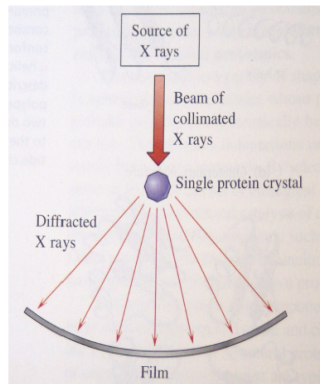
1 Phase Retrieval

- Classical Phase Retrieval
- Ptychographic Phase Retrieval
- PhaseLift
- PhaseCut
- Wirtinger Flows
- Gauss-Newton Method

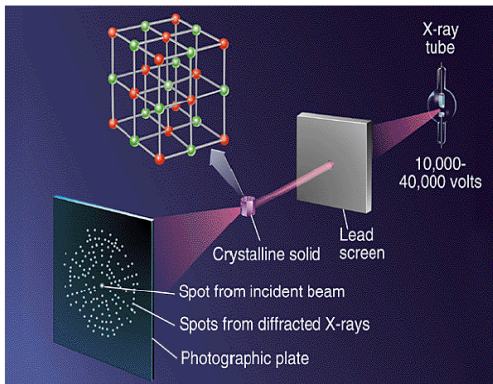
2 Cryo-Electron Microscopy

X-ray crystallography

Method for determining atomic structure within a crystal



principle



typical setup

10 Nobel Prizes in X-ray crystallography, and counting...

Missing phase problem

Detectors record **intensities** of diffracted rays \Rightarrow **phaseless data only!**



Fraunhofer diffraction \Rightarrow intensity of electrical \approx Fourier transform

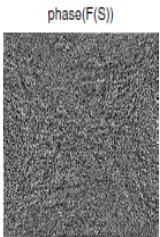
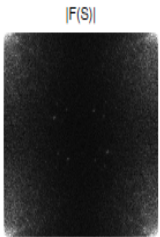
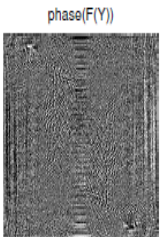
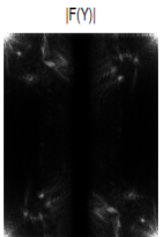
$$|\hat{x}(f_1, f_2)|^2 = \left| \int x(t_1, t_2) e^{-i2\pi(f_1 t_1 + f_2 t_2)} dt_1 dt_2 \right|^2$$

Electrical field $\hat{x} = |\hat{x}|e^{i\phi}$ with intensity $|\hat{x}|^2$

Phase retrieval problem (inversion)

How can we recover the phase (or signal $x(t_1, t_2)$) from $|\hat{x}(f_1, f_2)|$

Phase and magnitude



Phase carries more information than magnitude

Phase retrieval in X-ray crystallography

Knowledge of phase crucial to build electron density map

Algorithmic means of recovering phase structure without sophisticated setups

- Sayre ('52), Fienup ('78)
- Initial success in certain cases by using very specific prior knowledge



H. Hauptman

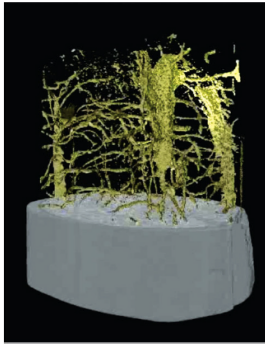


J. Karle

X-ray imaging: now and then



Röntgen (1895)



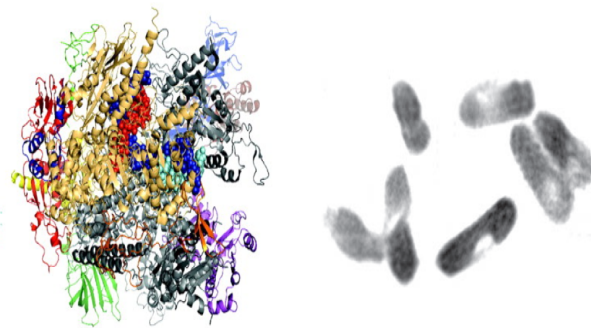
Dierolf (2010)

Need for lens-less imaging

Resurgence: imaging with new X-ray sources (undulators and synchrotrons); e.g. Miao and collaborators ('99—present)

X-ray diffraction microscopy

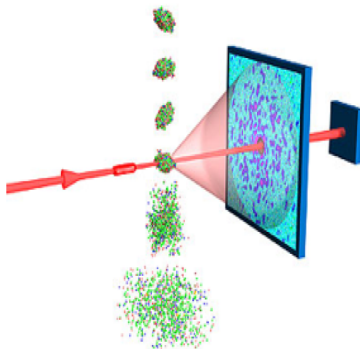
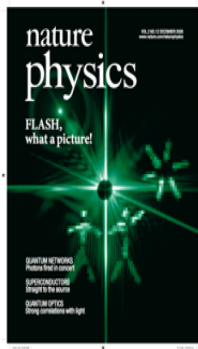
Imaging non-crystalline objects by measuring X-ray diffraction patterns using extremely intense and ultrashort X-ray pulses



Consequences

- PR problem getting more important
- Far less prior knowledge about unknown signal

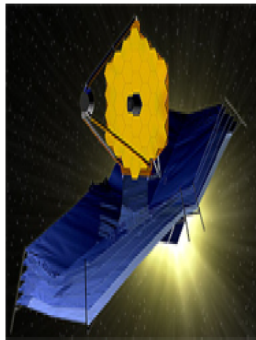
Ultrashort X-ray pulses



Other applications of phase retrieval



Hubble telescope



James Webb space telescope

Outline

1 Phase Retrieval

- Classical Phase Retrieval
- Ptychographic Phase Retrieval
- PhaseLift
- PhaseCut
- Wirtinger Flows
- Gauss-Newton Method

2 Cryo-Electron Microscopy

Classical Phase Retrieval

Feasibility problem

find $x \in S \cap \mathcal{M}$ or find $x \in S_+ \cap \mathcal{M}$

- given Fourier magnitudes:

$$\mathcal{M} := \{x(r) \mid |\hat{x}(\omega)| = b(\omega)\}$$

where $\hat{x}(\omega) = \mathcal{F}(x(r))$, \mathcal{F} : Fourier transform

- given support estimate:

$$S := \{x(r) \mid x(r) = 0 \text{ for } r \notin D\}$$

or

$$S_+ := \{x(r) \mid x(r) \geq 0 \text{ and } x(r) = 0 \text{ if } r \notin D\}$$

Error Reduction

Alternating projection:

$$x^{k+1} = \mathcal{P}_{\mathcal{S}}\mathcal{P}_{\mathcal{M}}(x^k)$$

- projection to \mathcal{S} :

$$\mathcal{P}_{\mathcal{S}}(x) = \begin{cases} x(r), & \text{if } r \in D, \\ 0, & \text{otherwise,} \end{cases}$$

- projection to \mathcal{M} :

$$\mathcal{P}_{\mathcal{M}}(x) = \mathcal{F}^*(\hat{y}), \text{ where } \hat{y} = \begin{cases} b(\omega) \frac{\hat{x}(\omega)}{|\hat{x}(\omega)|}, & \text{if } \hat{x}(\omega) \neq 0, \\ b(\omega), & \text{otherwise,} \end{cases}$$

Summary of projection algorithms

- Basic input-output (BIO)

$$x^{k+1} = (\mathcal{P}_{\mathcal{S}} \mathcal{P}_{\mathcal{M}} + I - \mathcal{P}_{\mathcal{M}}) (x^k)$$

- Hybrid input-output (HIO)

$$x^{k+1} = ((1 + \beta) \mathcal{P}_{\mathcal{S}} \mathcal{P}_{\mathcal{M}} + I - \mathcal{P}_{\mathcal{S}} - \beta \mathcal{P}_{\mathcal{M}}) (x^k)$$

- Hybrid projection reflection (HPR)

$$x^{k+1} = ((1 + \beta) \mathcal{P}_{\mathcal{S}_+} \mathcal{P}_{\mathcal{M}} + I - \mathcal{P}_{\mathcal{S}_+} - \beta \mathcal{P}_{\mathcal{M}}) (x^k)$$

- Relaxed averaged alternating reflection (RAAR)

$$x^{k+1} = (2\beta \mathcal{P}_{\mathcal{S}_+} \mathcal{P}_{\mathcal{M}} + \beta I - \beta \mathcal{P}_{\mathcal{S}_+} + (1 - 2\beta) \mathcal{P}_{\mathcal{M}}) (x^k)$$

- Difference map (DF)

$$x^{k+1} = (I + \beta(\mathcal{P}_{\mathcal{S}}((1 - \gamma_2) \mathcal{P}_{\mathcal{M}} - \gamma_2 I) + \mathcal{P}_{\mathcal{M}}((1 - \gamma_1) \mathcal{P}_{\mathcal{S}} - \gamma_1 I))) (x^k)$$

Consider problem

find x and y , such that $x = y$, $x \in \mathcal{X}$ and $y \in \mathcal{Y}$

- \mathcal{X} is either \mathcal{S} or \mathcal{S}_+ , and \mathcal{Y} is \mathcal{M} .
- Augmented Lagrangian function

$$\mathcal{L}(x, y, \lambda) := \lambda^\top(x - y) + \frac{1}{2}\|x - y\|^2$$

- ADMM:

$$x^{k+1} = \arg \min_{x \in \mathcal{X}} \mathcal{L}(x, y^k, \lambda^k),$$

$$y^{k+1} = \arg \min_{y \in \mathcal{Y}} \mathcal{L}(x^{k+1}, y, \lambda^k),$$

$$\lambda^{k+1} = \lambda^k + \beta(x^{k+1} - y^{k+1}),$$

- ADMM

$$\begin{aligned}x^{k+1} &= \mathcal{P}_{\mathcal{X}}(y^k - \lambda^k), \\y^{k+1} &= \mathcal{P}_{\mathcal{Y}}(x^{k+1} + \lambda^k), \\\lambda^{k+1} &= \lambda^k + \beta(x^{k+1} - y^{k+1}),\end{aligned}$$

- ADMM is equivalent to HIO or HPR

- if $\mathcal{P}_{\mathcal{X}}(x + y) = \mathcal{P}_{\mathcal{X}}(x) + \mathcal{P}_{\mathcal{X}}(y)$

$$x^{k+2} + \lambda^{k+1} = [(1 + \beta)\mathcal{P}_{\mathcal{X}}\mathcal{P}_{\mathcal{Y}} + (I - \mathcal{P}_{\mathcal{X}}) - \beta\mathcal{P}_{\mathcal{Y}}](x^{k+1} + \lambda^k)$$

Hybrid input-output (HIO)

$$x^{k+1} = ((1 + \beta)\mathcal{P}_{\mathcal{S}}\mathcal{P}_{\mathcal{M}} + I - \mathcal{P}_{\mathcal{S}} - \beta\mathcal{P}_{\mathcal{M}})(x^k)$$

- if $\beta = 1$

- ADMM: updating Lagrange Multiplier twice

$$x^{k+1} := \mathcal{P}_{\mathcal{X}}(y^k - \pi^k),$$

$$\pi^{k+1} := \pi^k + \beta(x^{k+1} - y^k) = -(I - \beta\mathcal{P}_{\mathcal{X}})(y^k - \pi^k),$$

$$y^{k+1} := \mathcal{P}_{\mathcal{Y}}(x^{k+1} + \lambda^k),$$

$$\lambda^{k+1} := \lambda^k + \nu(x^{k+1} - y^{k+1}) = (I - \nu\mathcal{P}_{\mathcal{Y}})(x^{k+1} + \lambda^k),$$

- ADMM is equivalent to ER if $\beta = \nu = 1$

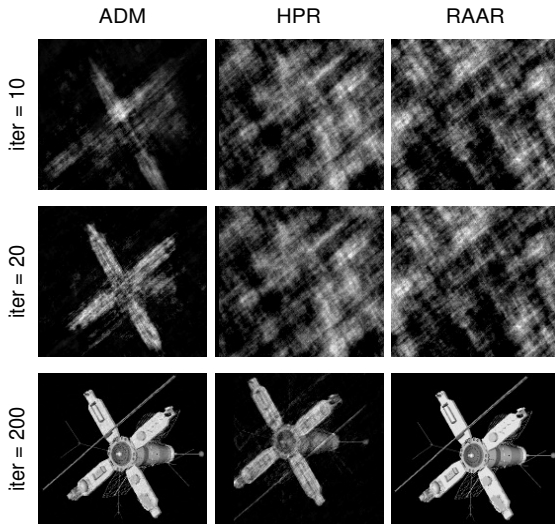
$$x^{k+1} := \mathcal{P}_{\mathcal{X}}(y^k) \text{ and } y^{k+1} := \mathcal{P}_{\mathcal{Y}}(x^{k+1}).$$

- ADMM is equivalent to BIO if $\beta = \nu = 1$

$$x^{k+1} + \lambda^k = (\mathcal{P}_{\mathcal{X}}\mathcal{P}_{\mathcal{Y}} + I - \mathcal{P}_{\mathcal{Y}})(x^k + \lambda^{k-1})$$

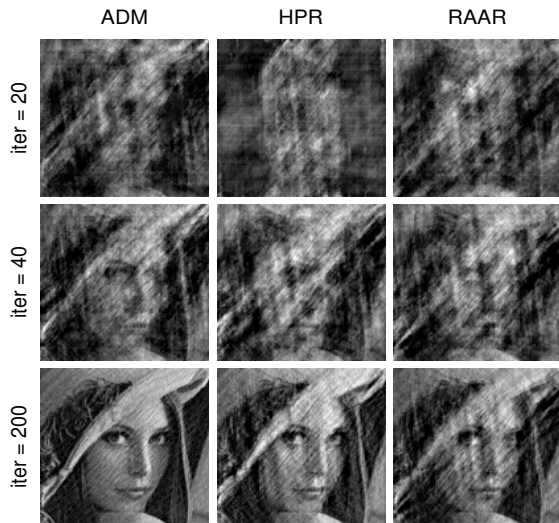
Numerical comparison

The parameter β in HPR and RAAR was updated dynamically with $\beta_0 = 0.95$. For ADMM, $\beta = 0.5$.



Numerical comparison

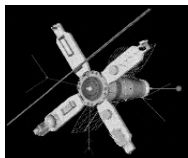
The parameter β in HPR and RAAR was updated dynamically with $\beta_0 = 0.95$. For ADMM, $\beta = 0.5$.



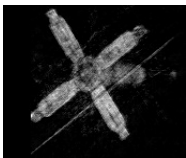
Numerical comparison

The parameter β was fixed at 0.6, 0.8 and 0.95 for the first, second and third rows respectively.

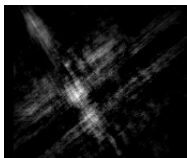
ADM



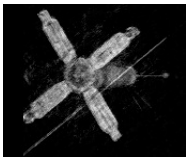
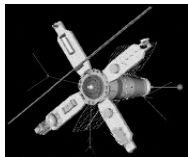
HPR



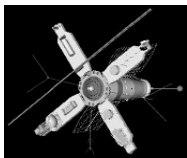
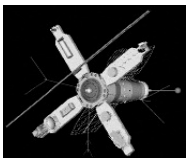
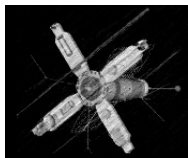
RAAR



ADM

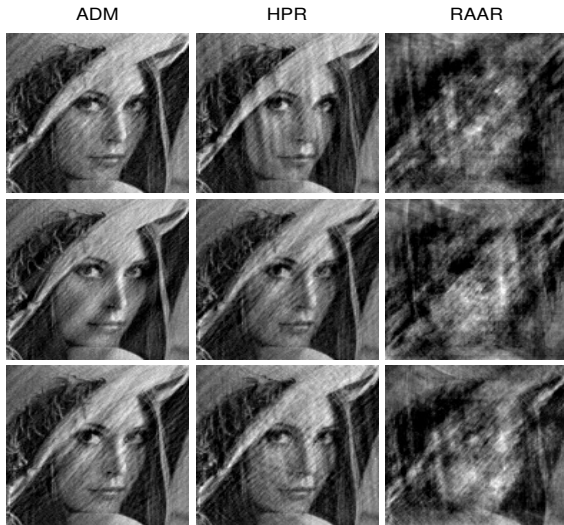


ADM



Numerical comparison

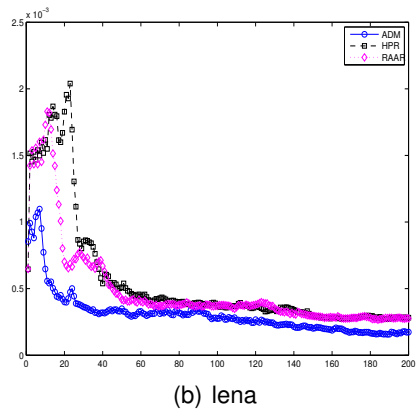
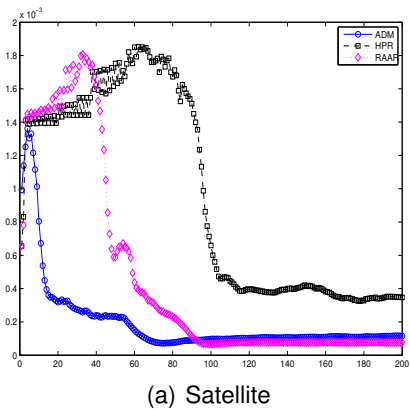
The parameter β was fixed at 0.6, 0.8 and 0.95 for the first, second and third rows respectively.



Numerical Results

Convergence behavior:

$$\text{err}^k = \frac{\|\mathcal{P}_{\mathcal{X}}(\mathcal{P}_{\mathcal{Y}}(x^k)) - \mathcal{P}_{\mathcal{Y}}(x^k)\|_F}{\|m\|_F}$$



Outline

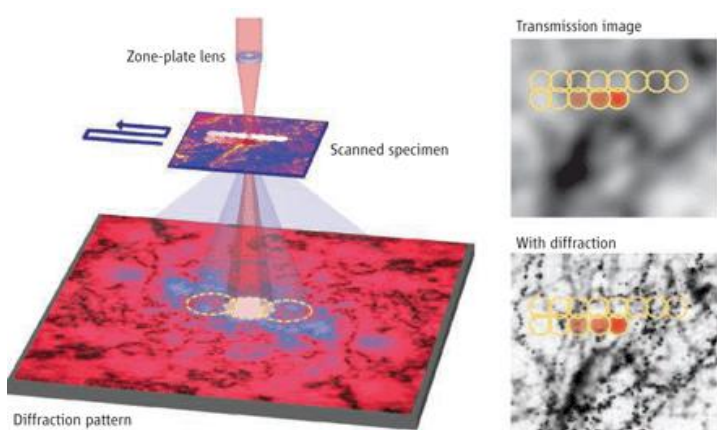
1 Phase Retrieval

- Classical Phase Retrieval
- **Ptychographic Phase Retrieval**
- PhaseLift
- PhaseCut
- Wirtinger Flows
- Gauss-Newton Method

2 Cryo-Electron Microscopy

Ptychographic Phase Retrieval

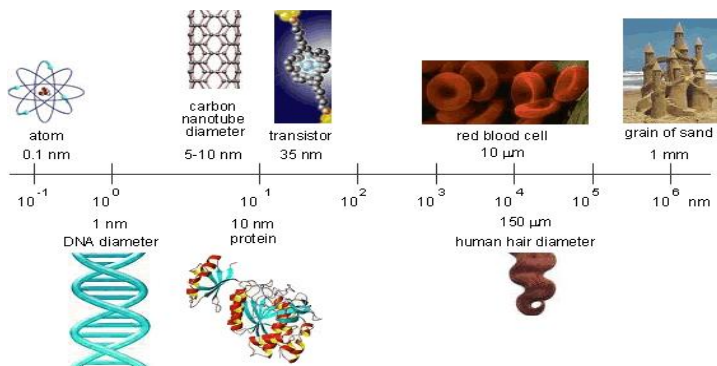
Given $|\mathcal{F}(Q_i\psi)|$ for $i = 1, \dots, k$, can we recover ψ ?



Ptychographic imaging along with advances in detectors and computing have resulted in X-ray microscopes with increased spatial resolution without the need for lenses

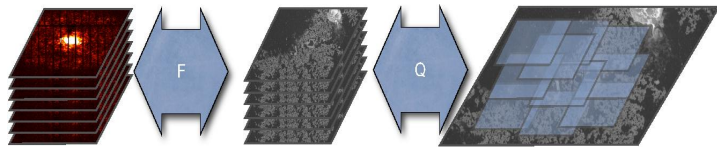
Ptychographic Phase Retrieval

- Nanoporous structure of shale, Toxicity of silver nanoparticles, Nano-scale properties of concrete, Bone and high strength nano-composite materials, Chemical structure of 3D polymeric materials for energy applications, Nanoscale structure of rocks related to carbon sequestration



Ptychographic Phase Retrieval

$$\left(\begin{array}{c} | \\ z \end{array} \right) = \left(\begin{array}{c} \mathcal{F} \\ \mathcal{F} \\ \mathcal{F} \\ \mathcal{F} \\ \mathcal{F} \end{array} \right) \left(\begin{array}{c} | \\ w \end{array} \right) \left(\begin{array}{c} | \\ \psi \end{array} \right)$$



Ptychographic Phase Retrieval

- given an object ψ , the illuminated portion:

$$x_i = Q_i \psi$$

- Q_i is an $m \times n$ illumination matrix: contains at least one nonzero row, and each row of Q_i contains at most one nonzero element.
- measurements:

$$b_i = |\mathcal{F}x_i| = |\mathcal{F}Q_i\psi|, \quad i = 1, 2, \dots, k,$$

- retrieving the phases of x_i from b_i
- x_i are not completely independent due to the overlap

Ptychographic Phase Retrieval

- Define: $x \equiv (x_1^*, x_2^*, \dots, x_k^*)^*$, $b \equiv (b_1^\top, b_2^\top, \dots, b_k^\top)^\top$,
 $Q \equiv (Q_1^*, Q_2^*, \dots, Q_k^*)^*$, and $\widehat{\mathcal{F}} \equiv \text{Diag}(\mathcal{F}, \mathcal{F}, \dots, \mathcal{F})$
- projections:

$$\mathcal{P}_Q = Q(Q^*Q)^{-1}Q^* \text{ and } \mathcal{P}_F(x) = \widehat{\mathcal{F}}^* \frac{\widehat{\mathcal{F}}x}{|\widehat{\mathcal{F}}x|} \cdot b,$$

- then we can apply projection algorithms

Reformulation

- reconstruct ψ from measures

$$b_i = |\mathcal{F}Q_i\psi|, \quad i = 1, 2, \dots, k,$$

Q_i is an $m \times n$ illumination matrix

- optimization problem

$$\min \rho(\psi) := \sum_{i=1}^k \frac{1}{2} \| |\mathcal{F}Q_i\psi| - b_i \|_2^2$$

- Reformulation:

$$\min \sum_{i=1}^k \frac{1}{2} \| |z_i| - b_i \|_2^2, \text{ s.t. } z_i = \mathcal{F}Q_i\psi, \quad i = 1, \dots, k$$

- Augmented Lagrangian function

$$\mathcal{L}(z_i, \psi, y_i) = \sum_{i=1}^k \left(\frac{1}{2} \| |z_i| - b_i \|_2^2 + y_i^* (\mathcal{F} Q_i \psi - z_i) + \frac{\alpha}{2} \| \mathcal{F} Q_i \psi - z_i \|_2^2 \right)$$

- z -subproblem:

$$(z_i^+)_{(l)} = \begin{cases} \frac{|(s_i)_{(l)}| + (b_i)_{(l)}}{(1+\alpha)|(s_i)_{(l)}|} (s_i)_{(l)}, & \text{if } (s_i)_{(l)} \neq 0 \text{ and } (b_i)_{(l)} > 0; \\ \pm \frac{(b_i)_{(l)}}{1+\alpha}, & \text{if } (s_i)_{(l)} = 0 \text{ and } (b_i)_{(l)} > 0; \\ 0, & \text{otherwise.} \end{cases}$$

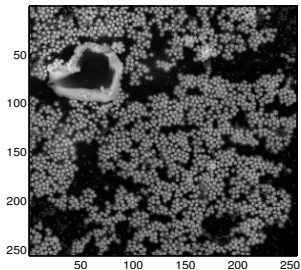
where $s_i = y_i + \alpha \mathcal{F} Q_i \psi$, $i = 1, \dots, k$

- ψ -subproblem:

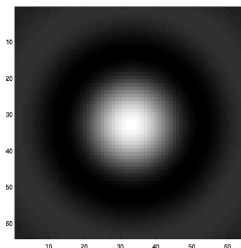
$$\psi^+ = \frac{1}{\alpha} \left(\sum_{i=1}^k Q_i^* Q_i \right)^{-1} \sum_{i=1}^k Q_i^* \mathcal{F}^* (\alpha z_i^+ - y_i)$$

Numerical Results

- Q_i is a 64×64 matrix
- the probe is translated by 16 pixels

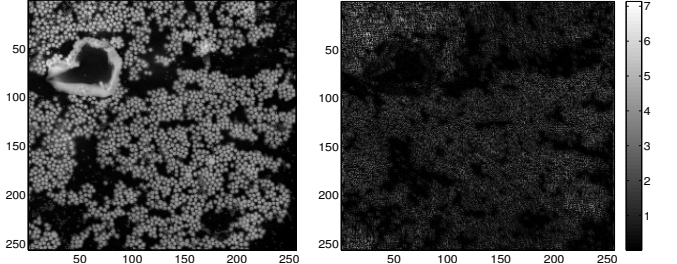


(a) The amplitude of the “gold ball” image.



(b) The amplitude of the probe.

Numerical Results



(a) The ADMM reconstruc-
tion.

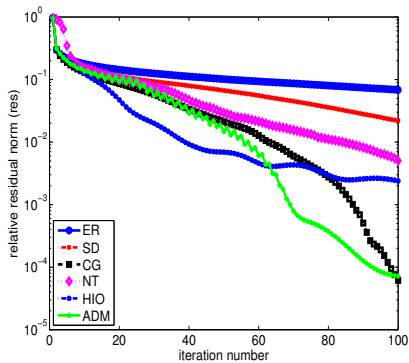
(b) The magnitude of the er-
ror produced by ADMM.

Numerical Results

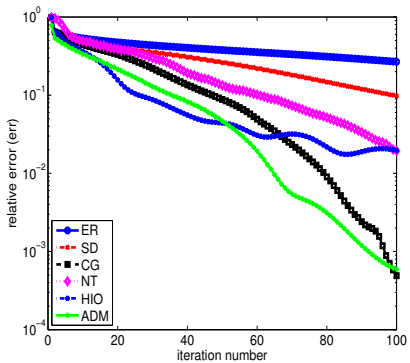
relative residual norm and relative error:

$$\text{res} = \frac{\sqrt{\sum_{i=1}^k \|z_i^j - b_i\|^2}}{\sqrt{\sum_{i=1}^k \|b_i\|^2}}, \quad err = \frac{\|c\psi^j - \psi\|}{\|\hat{\psi}\|},$$

where c is constant phase factor chosen to minimize $\|c\psi^j - \psi\|$.



(a) Change of the relative residual norm (res)



(b) Change of the relative error (err)

Outline

1 Phase Retrieval

- Classical Phase Retrieval
- Ptychographic Phase Retrieval
- **PhaseLift**
- PhaseCut
- Wirtinger Flows
- Gauss-Newton Method

2 Cryo-Electron Microscopy

Discrete mathematical model

- Phaseless measurements about $x_0 \in \mathbf{C}^n$

$$b_k = |\langle a_k, x_0 \rangle|^2, \quad k \in \{1, \dots, m\}$$

- Phase retrieval is feasibility problem

find x

$$\text{s.t. } |\langle a_k, x_0 \rangle|^2 = b_k, k = 1, \dots, m$$

Solving quadratic equations is NP-complete in general

NP-complete stone problem

Given weights $w_i \in \mathbb{R}$, $i = 1, \dots, n$, is there an assignment $x_i = \pm 1$ such that

$$\sum_{i=1}^n w_i x_i = 0?$$

Formulation as a quadratic system

$$\begin{aligned}|x_i|^2 &= 1, \quad i = 1, \dots, n \\ \left| \sum_{i=1}^n w_i x_i \right|^2 &= 0\end{aligned}$$

PhaseLift (C., Eldar, Strohmer, Voroninski, 2011)

Lifting: $X = xx^*$

$$b_k = |\langle a_k, x_0 \rangle|^2 = a_k^* x x^* a_k = \langle a_k a_k^*, X \rangle$$

Turns quadratic measurements into linear measurements $b = \mathcal{A}(X)$ about xx^*

Phase retrieval problem

$$\begin{aligned} & \text{find } X \\ & \text{s.t. } \mathcal{A}(X) = b \\ & \quad X \succeq 0, \text{rank}(X) = 1 \end{aligned}$$

PhaseLift

$$\begin{aligned} & \text{find } X \\ & \text{s.t. } \mathcal{A}(X) = b \\ & \quad X \succeq 0 \end{aligned}$$

Connections: relaxation of quadratically constrained QP's

- Shor (87) [Lower bounds on nonconvex quadratic optimization problems]
- Goemans and Williamson (95) [MAX-CUT]
- Chai, Moscoso, Papanicolaou (11)

Exact generalized phase retrieval via SDP

Phase retrieval problem

$$\begin{aligned} & \text{find } x \\ \text{s.t. } & b_k = |\langle a_k, x_0 \rangle|^2 \end{aligned}$$

PhaseLift

$$\begin{aligned} & \text{find } \text{tr}(X) \\ \text{s.t. } & \mathcal{A}(X) = b, \quad X \succeq 0 \end{aligned}$$

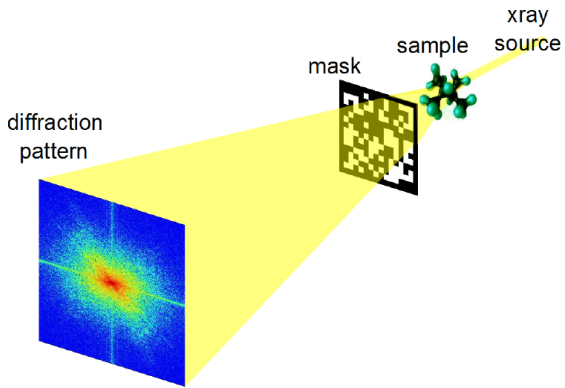
Theorem (C. and Li ('12); C., Strohmer and Voroninski ('11))

- ▶ a_k independently and uniformly sampled on unit sphere
- ▶ $m \gtrsim n$

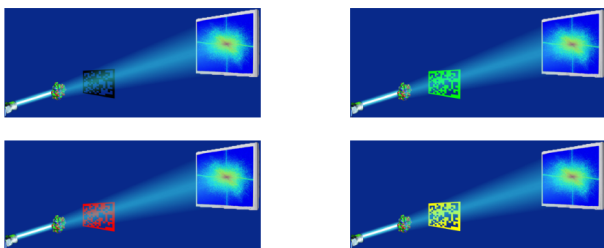
Then with prob. $1 - O(e^{-\gamma m})$, only feasible point is xx^*

$$\{X : \mathcal{A}(X) = b, \text{ and } X \succeq 0\} = \{xx^*\}$$

Extensions to physical setups



Coded diffraction

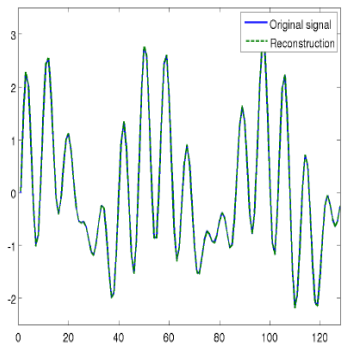


Collect diffraction patterns of modulated samples

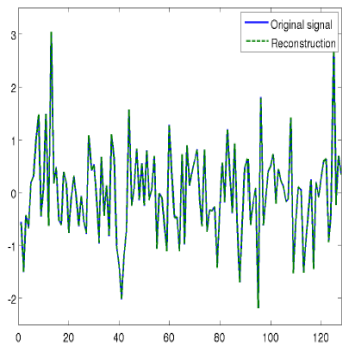
$$|\mathcal{F}(w[t]x[t])|^2 \quad w \in \mathcal{W}$$

Makes problem well-posed (for some choices of \mathcal{W})

Exact recovery



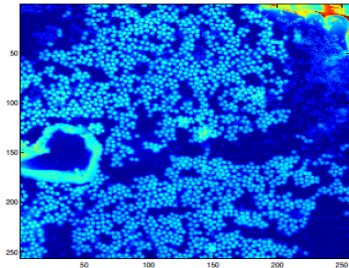
(a) Smooth signal (real part)



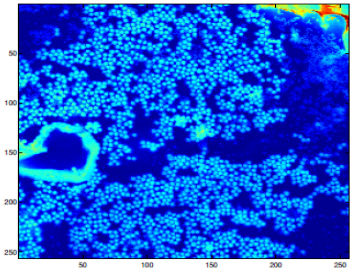
(b) Random signal (real part)

Figure: Recovery from 6 random binary masks

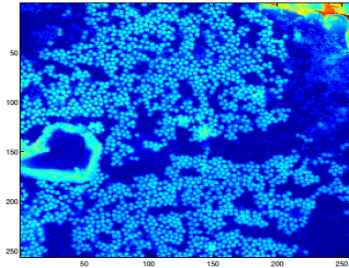
Numerical results: noiseless 2D images



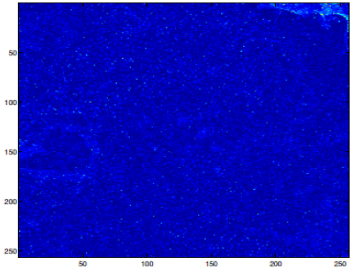
original image



3 Gaussian masks



8 binary masks



error with 8 binary masks

Outline

1 Phase Retrieval

- Classical Phase Retrieval
- Ptychographic Phase Retrieval
- PhaseLift
- **PhaseCut**
- Wirtinger Flows
- Gauss-Newton Method

2 Cryo-Electron Microscopy

PhaseCut

- Given $A \in \mathbf{C}^{m \times n}$ and $b \in \mathbb{R}^m$

find x , s.t. $|Ax| = b$.

(Candes et al. 2011b, Alexandre d'Aspremont 2013)

- An equivalent model

$$\min_{x \in \mathbf{C}^n, y \in \mathbb{R}^m} \frac{1}{2} \|Ax - y\|_2^2$$

s.t. $|y| = b$.

PhaseCut

- Reformulation:

$$\begin{aligned} & \min_{x \in \mathbb{C}^n, u \in \mathbb{C}^m} \frac{1}{2} \|Ax - \text{diag}(b)u\|_2^2 \\ & \text{s.t. } |u_i| = 1, , i = 1, \dots, m. \end{aligned}$$

- Given u , the signal variable is $x = A^\dagger \text{diag}(b)u$. Then

$$\begin{aligned} & \min_{u \in \mathbb{C}^m} u^* M u \\ & \text{s.t. } |u_i| = 1, i = 1, \dots, m, \end{aligned}$$

where $M = \text{diag}(b)(I - AA^\dagger)\text{diag}(b)$ is positive semidefinite.

- The MAXCUT problem

$$\begin{aligned} & \min_{U \in S_m} \text{Tr}(UM) \\ & \text{s.t. } U_{ii} = 1, i = 1, \dots, m, U \succeq 0. \end{aligned}$$

Outline

1 Phase Retrieval

- Classical Phase Retrieval
- Ptychographic Phase Retrieval
- PhaseLift
- PhaseCut
- **Wirtinger Flows**
- Gauss-Newton Method

2 Cryo-Electron Microscopy

Discrete mathematical model

Solve the equations:

$$y_r = |\langle a_r, x \rangle|^2, \quad r = 1, 2, \dots, m. \quad (1)$$

- **Gaussian model:**

$$a_r \in \mathbb{C}^n \stackrel{i.i.d.}{\sim} \mathcal{N}(0, I/2) + i\mathcal{N}(0, I/2).$$

- **Coded Diffraction model:**

$$y_r = \left| \sum_{t=0}^{n-1} x[t] \bar{d}_l(t) e^{-i2\pi kt/n} \right|^2, \quad r = (l, k), \quad 0 \leq k \leq n-1, \quad 1 \leq l \leq L.$$

Phase retrieval by non-convex optimization

Nonlinear least square problem:

$$\min_{z \in \mathbb{C}^n} f(z) = \frac{1}{4m} \sum_{k=1}^m (y_k - |\langle a_k, z \rangle|^2)^2$$

- Pro: operates over vectors and not matrices
- Con: f is nonconvex, many local minima

Strategies:

- Start from a sufficiently accurate initialization
- Make use of **Wirtinger derivative**

$$f(z) = \frac{1}{4m} \sum_{k=1}^m (y_k - |\langle a_k, z \rangle|^2)^2$$
$$\nabla f(z) = \frac{1}{m} \sum_{k=1}^m (|\langle a_k, z \rangle|^2 - y_k)(a_k a_k^*)z$$

- Careful iterations to avoid local minima

Algorithm: Gaussian model

- **Spectral Initialization:**

- 1 Input measurements $\{a_r\}$ and observation $\{y_r\}$ ($r = 1, 2, \dots, m$).
- 2 Calculate z_0 to be the leading eigenvector of $Y = \frac{1}{m} \sum_{r=1}^m y_r a_r a_r^*$.
- 3 Normalize z_0 such that $\|z_0\|^2 = n \frac{\sum_r y_r}{\sum_r \|a_r\|^2}$.

- **Iteration via Wirtinger derivatives:** for $\tau = 0, 1, \dots$

$$z_{\tau+1} = z_\tau - \frac{\mu_{\tau+1}}{\|z_0\|^2} \nabla f(z_\tau)$$

Convergence property: Gaussian model

distance (up to global phase)

$$\mathbf{dist}(z, \mathbf{x}) = \arg \min_{\pi \in [0, 2\pi]} \|z - e^{i\phi} \mathbf{x}\|$$

Theorem

Convergence for Gaussian model (C. Li and Soltanolkotabi ('14))

- number of samples $m \gtrsim n \log n$
- Step size $\mu \leq c/n$ ($c > 0$)

Then with probability at least $1 - 10e^{-\gamma n} - 8/n^2 - me^{-1.5n}$, we have $\text{dist}(z_0, \mathbf{x}) \leq \frac{1}{8} \|\mathbf{x}\|$ and after τ iteration

$$\mathbf{dist}(z_\tau, \mathbf{x}) \leq \frac{1}{8} \left(1 - \frac{\mu}{4}\right)^{\tau/2} \|\mathbf{x}\|.$$

Here γ is a positive constant.

Algorithm: Coded diffraction model

- **Initialization via resampled Wirtinger Flow:**

- 1 Input measurements $\{a_r\}$ and observation $\{y_r\} (r = 1, 2, \dots, m)$.
- 2 Divide the measurements and observations equally into $B + 1$ groups of size m' .
The measurements and observations in group b are denoted as $a_r^{(b)}$ and $y_r^{(b)}$ for $b = 0, 1, \dots, B$.
- 3 Obtain u_0 by conducting the spectral initialization on group 0.
- 4 For $b = 0$ to $B - 1$, perform the following update:

$$u_{b+1} = u_b - \frac{\mu}{\|u_0\|^2} \left(\frac{1}{m'} \sum_{r=1}^{m'} \left(|z^* a_r^{(b+1)}|^2 - y_r^{(b+1)} \right) (a_r^{(b+1)} (a_r^{(b+1)})^*) z \right).$$

- 5 Set $z_0 = u_B$.

- **Same iterations as the Gaussian model:**

for $\tau = 0, 1, \dots$

$$z_{\tau+1} = z_\tau - \frac{\mu_{\tau+1}}{\|z_0\|^2} \nabla f(z_\tau)$$

Convergence property: coded diffraction model

Theorem

Convergence for CD model (C. Li and Soltanolkotabi ('14))

- $L \gtrsim (\log n)^4$
- Step size $\mu \leq c(c > 0)$

Then with probability at least $1 - (2L + 1)/n^3 - 1/n^2$, we have $\text{dist}(z_0, \mathbf{x}) \leq \frac{1}{8\sqrt{n}} \|\mathbf{x}\|$ and after τ iteration

$$\text{dist}(z_\tau, \mathbf{x}) \leq \frac{1}{8\sqrt{n}} \left(1 - \frac{\mu}{3}\right)^{\tau/2} \|\mathbf{x}\|.$$

Numerical results: 1D signals

Consider the following two kinds of signals:

- **Random low-pass signals:**

$$x[t] = \sum_{k=-(M/2-1)}^{M/2} (X_k + iY_k) e^{2\pi i(k-1)(t-1)/n},$$

with $M=n/8$ and X_k and Y_k are i.i.d. $\mathcal{N}(0, 1)$.

- **Random Gaussian signals:** where $x \in \mathbb{C}^n$ is a random complex Gaussian vector with i.i.d. entries of the form

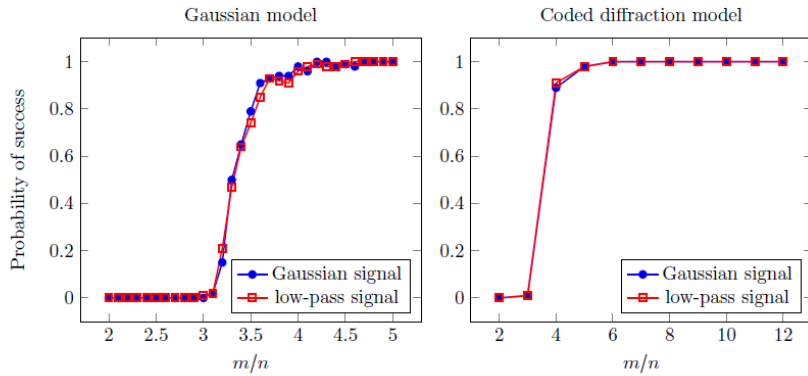
$$X[t] = X + iY,$$

with X and Y distributed as $\mathcal{N}(0, 1/2)$.

Success rate

- Set $n = 128$.
- Apply 50 iterations of the power method as initialization.
- Set the step length parameter $\mu_\tau = \min(1 - \exp(-\tau/\tau_0), 0.2)$, where $\tau_0 \approx 330$.
- Stop after 2500 iterations, and declare a trial successful if the relative error of the reconstruction $\text{dist}(\hat{x}, x)/\|x\|$ falls below 10^{-5} .
- The empirical probability of success is an average over 100 trials.

Success rate



Numerical results: natural images

- View RGB image as $n_1 \times n_2 \times 3$ array, and run the WF algorithm separately on each color band.
- Apply 50 iterations of the power method as initialization.
- Set the step length parameter $\mu_\tau = \min(1 - \exp(-\tau/\tau_0), 0.4)$, where $\tau_0 \approx 330$. Stop after 300 iterations.
- One FFT unit is the amount of time it takes to perform a single FFT on an image of the same size.

Numerical results: natural images



Figure: Naqsh-e Jahan Square, Esfahan. Image size is 189×768 pixels; timing is 61.4 sec or about 21200 FFT units. The relative error is 6.2×10^{-16} .

Numerical results: natural images



Figure: Stanford main quad. Image size is 320×1280 pixels; timing is 181.8120 sec or about 20700 FFT units. The relative error is 3.5×10^{-14} .

Numerical results: natural images



Figure: Milky way Galaxy. Image size is 1080×1920 pixels; timing is 1318.1 sec or 41900 FFT units. The relative error is 9.3×10^{-16} .

Recall the main theorems

Theorem

Convergence for Gaussian model (C. Li and Soltanolkotabi ('14))

- number of samples $m \gtrsim n \log n$
- Step size $\mu \leq c/n (c > 0)$

Then with probability at least $1 - 10e^{-\gamma n} - 8/n^2 - me^{-1.5n}$, we have
 $\text{dist}(z_0, \mathbf{x}) \leq \frac{1}{8} \|\mathbf{x}\|$ and after τ iteration

$$\text{dist}(z_\tau, \mathbf{x}) \leq \frac{1}{8} \left(1 - \frac{\mu}{4}\right)^{\tau/2} \|\mathbf{x}\|.$$

Here γ is a positive constant.

Recall the main theorems

Theorem

Convergence for CD model (C. Li and Soltanolkotabi ('14))

- $L \gtrsim (\log n)^4$
- Step size $\mu \leq c(c > 0)$

Then with probability at least $1 - (2L + 1)/n^3 - 1/n^2$, we have

$\text{dist}(z_0, \mathbf{x}) \leq \frac{1}{8\sqrt{n}} \|\mathbf{x}\|$ and after τ iteration

$$\text{dist}(z_\tau, \mathbf{x}) \leq \frac{1}{8\sqrt{n}} \left(1 - \frac{\mu}{3}\right)^{\tau/2} \|\mathbf{x}\|.$$

Regularity condition

Definition

Definition We say that the function f satisfies the regularity condition or $RC(\alpha, \beta, \epsilon)$ if for all vectors $z \in E(\epsilon)$ we have

$$Re \left(\langle \nabla f(z), z - xe^{i\phi(z)} \rangle \right) \geq \frac{1}{\alpha} dist^2(z, x) + \frac{1}{\beta} \|\nabla f(z)\|^2.$$

- $\phi(z) := \arg \min_{\phi \in [0, 2\pi]} \|z - e^{i\phi}x\|.$
- $dist(z, x) := \|z - e^{i\phi(z)}x\|.$
- $E(\epsilon) := \{z \in \mathbb{C}^n : dist(z, x) \leq \epsilon\}.$

Proof of convergence

Lemma 1

Assume that f obeys $RC((\alpha, \beta, \epsilon))$ for all $z \in E(\epsilon)$. Furthermore, suppose $z_0 \in E(\epsilon)$, and assume $0 < \mu \leq 2/\beta$. Consider the following update

$$z_{\tau+1} = z_\tau - \mu \nabla f(z_\tau).$$

Then for all τ we have $z_\tau \in E(\epsilon)$ and

$$\text{dist}^2(z_\tau, x) \leq \left(1 - \frac{2\mu}{\alpha}\right)^\tau \text{dist}^2(z_0, x).$$

Proof of convergence

Proof.

We prove that if $z \in E(\epsilon)$ then for all $0 < \mu \leq 2/\beta$

$$z_+ = z - \mu \nabla f(z)$$

obeys

$$\text{dist}^2(z_+, x) \leq \left(1 - \frac{2\mu}{\alpha}\right) \text{dist}^2(z, x).$$

Then the lemma holds by inductively applying the equation above.

Proof of convergence

Simple algebraic manipulations together with the regularity condition give

$$\begin{aligned}\|z_+ - xe^{i\phi(z)}\|^2 &= \|z - xe^{i\phi(z)} - \mu \nabla f(z)\|^2 \\&= \|z - xe^{i\phi(z)}\|^2 - 2\mu \operatorname{Re}(\langle \nabla f(z), z - xe^{i\phi(z)} \rangle) + \mu^2 \|\nabla f(z)\|^2 \\&\leq \|z - xe^{i\phi(z)}\|^2 - 2\mu \left(\frac{1}{\alpha} \|z - xe^{i\phi(z)}\|^2 + \frac{1}{\beta} \|\nabla f(z)\|^2 \right) \\&\quad + \mu^2 \|\nabla f(z)\|^2 \\&= \left(1 - \frac{2\mu}{\alpha}\right) \|z - xe^{i\phi(z)}\|^2 + \mu \left(\mu - \frac{2}{\beta}\right) \|\nabla f(z)\|^2 \\&\leq \left(1 - \frac{2\mu}{\alpha}\right) \|z - xe^{i\phi(z)}\|^2,\end{aligned}$$

which concludes the proof.

Proof of regularity condition

We will make use of the following lemma:

Lemma 2

- ① x is a solution obeying $\|x\| = 1$, and is independent from the sampling vectors;
- ② $m \geq c(\delta)n \log n$ in Gaussian model or $L \geq c(\delta) \log^3 n$ in CD model.

Then,

$$\|\nabla^2 f(x) - \mathbb{E} \nabla^2 f(x)\| \leq \delta$$

holds with probability at least $1 - 10e^{-\gamma n} - 8/n^2$ and $1 - (2L + 1)/n^3$ for the Gaussian and CD model, respectively.

- The concentration of the Hessian matrix at the optimizers.

Proof of regularity condition

Based on the lemma above with $\delta = 0.01$, we prove the regularity condition by establishing the local curvature condition and the local smoothness condition.

Local curvature condition

We say that the function f satisfies the local curvature condition or $LCC(\alpha, \epsilon, \delta)$ if for all vectors $z \in E(\epsilon)$,

$$Re \left(\langle \nabla f(z), z - xe^{i\phi(z)} \rangle \right) \geq \left(\frac{1}{\alpha} + \frac{1-\delta}{4} \right) dist^2(z, x) + \frac{1}{10m} \sum_{r=1}^m \left| a_r^*(z - xe^{i\phi(z)}) \right|^4.$$

The LCC condition states that the function curves sufficiently upwards along most directions near the curve of global optimizers.

For the CD model, LCC holds with $\alpha \geq 30$ and $\epsilon = \frac{1}{8\sqrt{n}}$;

For the Gaussian model, LCC holds with $\alpha \geq 8$ and $\epsilon = \frac{1}{8}$.

Proof of regularity condition

Local smoothness condition

We say that the function f satisfies the local smoothness condition or $LSC(\beta, \epsilon, \delta)$ if for all vectors $z \in E(\epsilon)$ we have

$$\|\nabla f(z)\|^2 \leq \beta \left(\frac{(1-\delta)}{4} dist^2(z, x) + \frac{1}{10m} \sum_{r=1}^m \left| a_r^*(z - xe^{i\phi(z)}) \right|^4 \right).$$

The LSC condition states that the gradient of the function is well behaved near the curve of global optimizers. Using $\delta = 0.01$, LSC holds with $\beta \geq 550 + 3n$

$$\beta \geq 550 \quad \text{for } \epsilon = 1/(8\sqrt{n}),$$

$$\beta \geq 550 + 3n \quad \text{for } \epsilon = 1/8.$$

Proof of regularity condition

In conclusion, when $\delta = 0.01$, for the Gaussian model, the regularity condition holds with

$$\alpha \geq 8, \beta \geq 550 + 3n, \text{ and } \epsilon = 1/8.$$

while for the CD model, the regularity condition holds with

$$\alpha \geq 30, \beta \geq 550, \text{ and } \epsilon = 1/(8\sqrt{n}),$$

Therefore, for the Gaussian model, linear convergence holds if the initial points satisfies $\text{dist}(z_0, x) \leq 1/8$; for the CD model, linear convergence holds if $\text{dist}(z_0, x) \leq 1/(8\sqrt{n})$.

Proof of initialization

Recall the initialization algorithm:

- 1 Input measurements $\{a_r\}$ and observation $\{y_r\} (r = 1, 2, \dots, m)$.
- 2 Calculate z_0 to be the leading eigenvector of $Y = \frac{1}{m} \sum_{r=1}^m y_r a_r a_r^*$.
- 3 Normalize z_0 such that $\|z_0\|^2 = n \frac{\sum_r y_r}{\sum_r \|a_r\|^2}$.

Ideas:

$$\mathbb{E} \left[\frac{1}{m} \sum_{r=1}^m y_r a_r a_r^* \right] = I + 2xx^*,$$

and any leading eigenvector of $I + 2xx^*$ is of the form λx . Therefore, by the strong law of large number, the initialization step would recover the direction of x perfectly as long as there are enough samples.

Proof of initialization

In the detailed proof, we will use the following lemma:

Lemma 3

In the setup of Lemma 2,

$$\left\| I - \frac{1}{m} \sum_{r=1}^m a_r a_r^* \right\| \leq \delta,$$

holds with probability at least $1 - 2e^{-\gamma m}$ for the Gaussian model and $1 - 1/n^2$ for the CD model. On this event,

$$(1 - \delta) \|h\|^2 \leq \frac{1}{m} \sum_{r=1}^m |a_r^* h|^2 \leq (1 + \delta) \|h\|^2$$

holds for all $h \in \mathbb{C}^n$.

Proof of initialization

Detailed proof:

Lemma 2 gives

$$\|Y - (xx^* + \|x\|^2 I)\| \leq \epsilon := 0.001.$$

Let \tilde{z}_0 be the unit eigenvector corresponding to the top eigenvalue λ_0 of Y , then

$$|\lambda_0 - (|\tilde{z}_0 x|^2 + 1)| = |\tilde{z}_0^* (Y - (xx^* + I)) \tilde{z}_0| \leq \|Y - (xx^* + I)\| \leq \epsilon.$$

Therefore, $|\tilde{z}_0^* x|^2 \geq \lambda_0 - 1 - \epsilon$. Meanwhile, since λ_0 is the top eigenvalue of Y , and $\|x\| = 1$, we have

$$\lambda_0 \geq x^* Y x = x^* (Y - (I + x^* x)) x + 2 \geq 2 - \epsilon.$$

Combining the above two inequalities together, we have

$$|\tilde{z}_0^* x|^2 \geq 1 - 2\epsilon \Rightarrow \text{dist}^2(\tilde{z}_0, x) \leq 2 - 2\sqrt{1 - 2\epsilon} \leq \frac{1}{256} \Rightarrow \text{dist}(\tilde{z}_0, x) \leq \frac{1}{16}.$$

Proof of initialization

Now consider the normalization. Recall that $z_0 = \left(\sqrt{\frac{1}{m} \sum_{r=1}^m |a_r^* x|^2} \right) \tilde{z}_0$. By Lemma 3, with high probability we have

$$|\|z_0\| - 1| \leq |\|z_0\|^2 - 1| = \left| \frac{1}{m} \sum_{r=1}^m |a_r^* x|^2 - 1 \right| \leq \delta < \frac{1}{16}.$$

Therefore, we have

$$\text{dist}(z_0, x) \leq \|z_0 - \tilde{z}_0\| + \text{dist}(\tilde{z}_0, x) \leq |\|z_0\| - 1| + \text{dist}(\tilde{z}_0, x) \leq \frac{1}{8}.$$

Proof of initialization: Resampled WF

Recall the initialization step via resampled Wirtinger flow:

- 1 Input measurements $\{a_r\}$ and observation $\{y_r\} (r = 1, 2, \dots, m)$.
- 2 Divide the measurements and observations equally into $B + 1$ groups of size m' . The measurements and observations in group b are denoted as $a_r^{(b)}$ and $y_r^{(b)}$ for $b = 0, 1, \dots, B$.
- 3 Obtain u_0 by conducting the spectral initialization on group 0.
- 4 For $b = 0$ to $B - 1$, perform the following update:

$$u_{b+1} = u_b - \frac{\mu}{\|u_0\|^2} \left(\frac{1}{m'} \sum_{r=1}^{m'} \left(|z^* a_r^{(b+1)}|^2 - y_r^{(b+1)} \right) (a_r^{(b+1)} (a_r^{(b+1)})^*) z \right).$$

- 5 Set $z_0 = u_B$.

Proof of initialization: Resampled WF

Outline of the proof:

- ① For step 3, by the result of Algorithm 1, u_0 obeys

$$dist(u_0, x) \leq \frac{1}{8}.$$

- ② For step 4, define $f(z; b) = \frac{1}{2m'} \sum_{r=1}^{m'} \left(|z_* a_r^{(b+1)}|^2 - y_r^{(b+1)} \right)^2$, then the update can be written as

$$u_{b+1} = u_b - \frac{\mu}{\|u_0\|^2} \nabla f(z; b).$$

We prove the linear convergence of this series of updates by verifying the following regularity condition:

$$Re \left(\langle \nabla f(z; b), z - xe^{i\phi(z)} \rangle \right) \geq \frac{1}{\tilde{\alpha}} dist^2(z, x) + \frac{1}{\tilde{\beta}} \|\nabla f(z; b)\|.$$

Outline

1 Phase Retrieval

- Classical Phase Retrieval
- Ptychographic Phase Retrieval
- PhaseLift
- PhaseCut
- Wirtinger Flows
- Gauss-Newton Method

2 Cryo-Electron Microscopy

Nonlinear least square problem

$$\min_{z \in \mathbb{C}^n} f(z) = \frac{1}{4m} \sum_{k=1}^m (y_k - |\langle a_k, z \rangle|^2)^2$$

Using Wirtinger derivative:

$$\mathbf{z} := \begin{bmatrix} z \\ \bar{z} \end{bmatrix};$$

$$g(z) := \nabla_c f(z) = \frac{1}{m} \sum_{r=1}^m (|a_r^T z|^2 - y_r) \begin{bmatrix} (a_r a_r^T) z \\ (\bar{a}_r a_r^T) \bar{z} \end{bmatrix};$$

$$J(z) := \frac{1}{\sqrt{m}} \sum_{r=1}^m \begin{bmatrix} |a_1^* z| a_1, & |a_2^* z| a_2, & \cdots, & |a_m^* z| a_m \\ |a_1^* z| \bar{a}_1, & |a_2^* z| \bar{a}_2, & \cdots, & |a_m^* z| \bar{a}_m \end{bmatrix}^T;$$

$$\Psi(z) := J(z)^T J(z) = \frac{1}{m} \sum_{r=1}^m \begin{bmatrix} |a_r^T z|^2 a_r a_r^T & (a_r^T z)^2 a_r a_r^T \\ (a_r^T z)^2 \bar{a}_r a_r^T & |a_r^T z|^2 \bar{a}_r a_r^T \end{bmatrix}.$$

The Modified LM method for Phase Retrieval

Levenberg-Marquardt Iteration:

$$\mathbf{z}_{k+1} = \mathbf{z}_k - (\Psi(z_k) + \mu_k I)^{-1} g(z_k)$$

Algorithm

- 1 Input:** Measurements $\{a_r\}$, observations $\{y_r\}$. Set $\epsilon \geq 0$.
- 2** Construct z_0 using the spectral initialization algorithms.
- 3 While** $\|g(z_k)\| \geq \epsilon$ **do**
 - Compute s_k by solving equation

$$\Psi_{z_k}^{\mu_k} s_k = (\Psi(z_k) + \mu_k I) s_k = -g(z_k).$$

until

$$\|\Psi_{z_k}^{\mu_k} s_k + g(z_k)\| \leq \eta_k \|g(z_k)\|.$$

- Set $\mathbf{z}_{k+1} = \mathbf{z}_k + s_k$ and $k := k + 1$.

- 3 Output:** z_k .

Convergence of the Gaussian Model

Theorem

If the measurements follow the Gaussian model, the LM equation is solved accurately ($\eta_k = 0$ for all k), and the following conditions hold:

- $m \geq cn \log n$, where c is sufficiently large;
- If $f(z_k) \geq \frac{\|z_k\|^2}{900n}$, let $\mu_k = 70000n\sqrt{nf(z_k)}$; if else, let $\mu_k = \sqrt{f(z_k)}$.

Then, with probability at least $1 - 15e^{-\gamma n} - 8/n^2 - me^{-1.5n}$, we have $\text{dist}(z_0, x) \leq (1/8)\|x\|$, and

$$\text{dist}(z_{k+1}, x) \leq c_1 \text{dist}(z_k, x),$$

Meanwhile, once $f(z_s) < \frac{\|z_s\|^2}{900n}$, for any $k \geq s$ we have

$$\text{dist}(z_{k+1}, x) < c_2 \text{dist}(z_k, x)^2.$$

Convergence of the Gaussian Model

In the theorem above,

$$c_1 := \begin{cases} \left(1 - \frac{\|x\|}{4\mu_k}\right), & \text{if } f(z_k) \geq \frac{1}{900n} \|z_k\|^2; \\ \frac{4.28 + 5.56\sqrt{n}}{9.89\sqrt{n}}, & \text{otherwise.} \end{cases}$$

and

$$c_2 = \frac{4.28 + 5.56\sqrt{n}}{\|x\|}.$$

Key to proof

Lower bound of GN matrix's second smallest eigenvalue

For any $y, z \in \mathbb{C}^n$, $\text{Im}(y^*z) = 0$, we have:

$$\mathbf{y}^* \Psi(z) \mathbf{y} \geq \|y\|^2 \|z\|^2,$$

holds with high probability.

$$\text{Im}(y^*z) = 0 \Rightarrow \|(\Psi_z^\mu)^{-1} \mathbf{y}\| \leq \frac{2}{\|z\|^2 + \mu} \|\mathbf{y}\|.$$

Key to proof

Local error bound property

$$\frac{1}{4} \mathbf{dist}(z, x)^2 \leq f(z) \leq 8.04 \mathbf{dist}(z, x)^2 + 6.06n \mathbf{dist}(z, x)^4,$$

holds for any z satisfying $\mathbf{dist}(z, x) \leq \frac{1}{8}$.

Regularity condition

$$\mu(z) \mathbf{h}^* (\Psi_z^\mu)^{-1} g(\mathbf{z}) \geq \frac{1}{16} \|\mathbf{h}\|^2 + \frac{1}{64100n\|h\|} \|g(\mathbf{z})\|^2$$

holds for any $z = x + h$, $\|h\| \leq \frac{1}{8}$, and $f(z) \geq \frac{\|z\|^2}{900n}$.

Convergence for the inexact LM method

Theorem

Convergence of the inexact LM method for the Gaussian model:

- $m \gtrsim n \log n$;
- μ_k takes the same value as in the exact LM method for the Gaussian model;
- $\eta_k \leq \frac{(1-c_1)\mu_k}{25.55n\|z_k\|}$ if $f(z_k) \geq \frac{\|z_k\|^2}{900n}$; otherwise $\eta_k \leq \frac{(4.33\sqrt{n}-4.28)\mu_k\|g_k\|}{372.54n^2\|z_k\|^3}$.

Then, with probability at least $1 - 15e^{-\gamma n} - 8/n^2 - me^{-1.5n}$, we have $\text{dist}(z_0, x) \leq \frac{1}{8}\|x\|$, and

$$\text{dist}(z_{k+1}, x) \leq \frac{1+c_1}{2} \text{dist}(z_k, x), \quad \text{for all } k = 0, 1, \dots$$

$$\text{dist}(z_{k+1}, x) \leq \frac{9.89\sqrt{n} + c_2\|x\|}{2\|x\|} \text{dist}(z_k, x)^2, \quad \text{for all } f(z_k) < \frac{\|z_k\|^2}{900n}.$$

Here c_1 and c_2 take the same values as in the exact algorithm for the Gaussian model.

Solving the LM Equation: PCG

Solve

$$(\Psi_k + \mu_k I)u = g_k$$

by Pre-conditioned Conjugate Gradient Method:

$$\mathbf{M}^{-1}(\Psi_k + \mu_k I)u = \mathbf{M}^{-1}g_k, \quad \mathbf{M} = \Phi_k + \mu_k I.$$

$$\Phi(z) := \begin{bmatrix} zz^* & 2zz^T \\ 2\bar{z}z^* & \bar{z}z^T \end{bmatrix} + \|z\|^2 I_{2n}$$

- **small condition number**
- **Easy to inverse:** $M = (\mu_k + \|z_k\|^2)I + M_1$, where M_1 is rank-2 matrix.

Solving the LM Equation: PCG

- small condition number.

Lemma

Consider solving the equation $(\Phi_z^\mu)^{-1}\Psi_z^\mu s = (\Phi_z^\mu)^{-1}g(\mathbf{z})$ by the CG method from $s_0 := -(\Phi_z^\mu)^{-1}g(\mathbf{z})$. Let s_* be the solution of the system. Define $V := \{\mathbf{x} : \mathbf{x} = [x^*, x^T]^*, x \in \mathbb{C}^n\}$. Then, V is an invariant subspace of $(\Phi_z^\mu)^{-1}\Psi_z^\mu$, and $s_0, s_* \in V$. Meanwhile, choosing $\mu_k = Kn\sqrt{f(z)}$, then the eigenvalues of $(\Phi_z^\mu)^{-1}\Psi_z^\mu$ on V satisfy:

$$1 - \frac{57}{K\sqrt{n}} \leq \lambda \leq 1 + \frac{57}{K\sqrt{n}}.$$

Solving the LM Equation: PCG

- Easy to inverse.

Calculate by Sherman-Morrison-Woodbury theorem:

$$(\Phi_z^\mu)^{-1} = aI_{2n} + b \begin{bmatrix} z \\ \bar{z} \end{bmatrix} [z^*, z^T] + c \begin{bmatrix} z \\ -\bar{z} \end{bmatrix} [z^*, -z^T]$$

where

$$a = \frac{1}{\|z\|^2 + \mu}, \quad b = -\frac{3}{2(\|z\|^2 + \mu)(4\|z\|^2 + \mu)}, \quad c = \frac{1}{2(\|z\|^2 + \mu)\mu}.$$

Outline

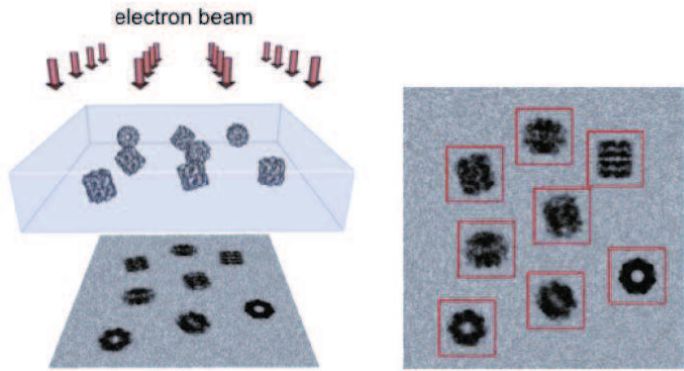
1 Phase Retrieval

- Classical Phase Retrieval
- Ptychographic Phase Retrieval
- PhaseLift
- PhaseCut
- Wirtinger Flows
- Gauss-Newton Method

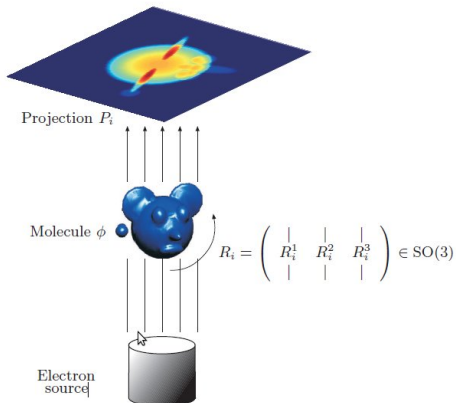
2 Cryo-Electron Microscopy

Single Particle Cryo-Electron Microscopy

Drawing of the imaging process:

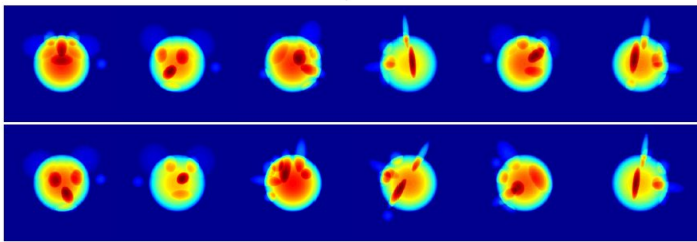
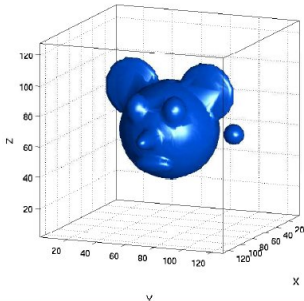


Single Particle Cryo-Electron Microscopy



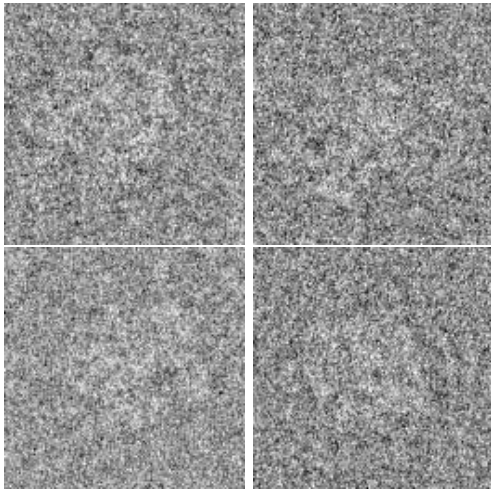
- Projection images $P_i(x, y) = \int_{-\infty}^{\infty} \phi(xR_i^1 + yR_i^2 + zR_i^3) dz + \text{"noise"}$.
- $\phi : \mathbb{R}^3 \rightarrow \mathbb{R}$ is the electric potential of the molecule.
- Cryo-EM problem: Find ϕ and R_1, \dots, R_n given P_1, \dots, P_n .

A Toy Example



E. coli 50S ribosomal subunit: sample images

Fred Sigworth, Yale Medical School



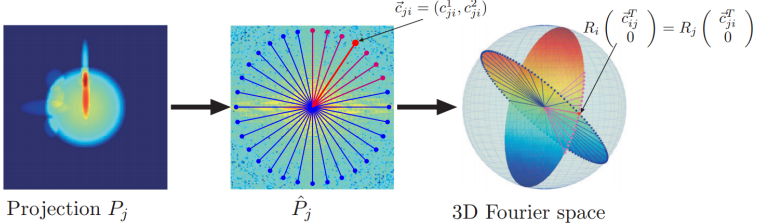
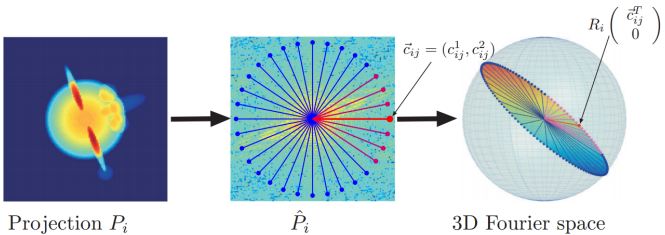
Algorithmic Pipeline

- Particle Picking: manual, automatic or experimental image segmentation.
- Class Averaging: classify images with similar viewing directions, register and average to improve their signal-to-noise ratio (SNR).
[S, Zhao, Shkolnisky, Hadani, SIIMS, 2011.](#)
- Orientation Estimation:
[S, Shkolnisky, SIIMS, 2011.](#)
- Three-dimensional Reconstruction:
a 3D volume is generated by a tomographic inversion algorithm.
- Iterative Refinement

What mathematics do we use to solve the problem?

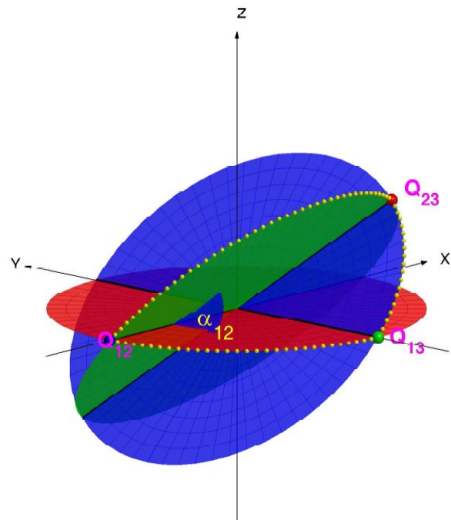
- Tomography
- Convex optimization and semidefinite programming
- Random matrix theory (in several places)
- Representation theory of $\text{SO}(3)$ (if viewing directions are uniformly distributed)
- Spectral graph theory, (vector) diffusion maps
- Fast randomized algorithms
- ...

Orientation Estimation: Fourier projection-slice



Angular Reconstruction

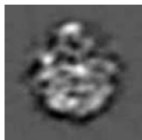
Van Heel 1987, Vainshtein and Goncharov 1986



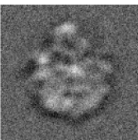
Experiments with simulated noisy projections

- Each projection is 129x129 pixels

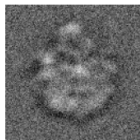
$$\text{SNR} = \frac{\text{Var}(\text{Signal})}{\text{Var}(\text{Noise})}$$



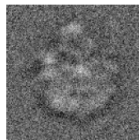
(a) Clean



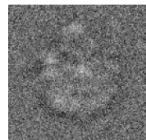
(b) $\text{SNR}=2^0$



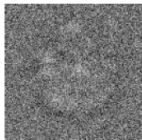
(c) $\text{SNR}=2^{-1}$



(d) $\text{SNR}=2^{-2}$



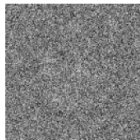
(e) $\text{SNR}=2^{-3}$



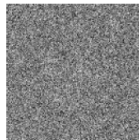
(f) $\text{SNR}=2^{-4}$



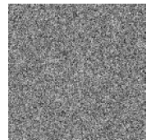
(g) $\text{SNR}=2^{-5}$



(h) $\text{SNR}=2^{-6}$



(i) $\text{SNR}=2^{-7}$



(j) $\text{SNR}=2^{-8}$

Detection of Common-lines between images

common line between two images P_i and P_j :

- radial resolution: n_r , angular resolution: n_θ
- Fourier transformed images: $(\vec{l}_0^k, \vec{l}_1^k, \dots, \vec{l}_{n_\theta-1}^k)$
- Compare $\vec{l}_0^i, \vec{l}_1^i, \dots, \vec{l}_{n_\theta-1}^i$ and $\vec{l}_0^j, \vec{l}_1^j, \dots, \vec{l}_{n_\theta-1}^j$
- maximum normalized cross correlation:

$$(m_{i,j}, m_{j,i}) = \arg \max_{0 \leq m_1 < n_\theta/2, 0 \leq m_2 < n_\theta} \frac{\langle \vec{l}_{m_1}^i, \vec{l}_{m_2}^j \rangle}{\| \vec{l}_{m_1}^i \| \| \vec{l}_{m_2}^j \|}, \text{ for all } i \neq j,$$

Least Squares Approach

- The directions of detected common-lines between \hat{P}_i and \hat{P}_j

$$\begin{aligned}\vec{c}_{ij} &= (c_{ij}^1, c_{ij}^2) = (\cos(2\pi m_{ij}/n_\theta), \sin(2\pi m_{ij}/n_\theta)), \\ \vec{c}_{ji} &= (c_{ji}^1, c_{ji}^2) = (\cos(2\pi m_{ji}/n_\theta), \sin(2\pi m_{ji}/n_\theta)).\end{aligned}$$

- $R_i \in \mathbf{SO}(3)$, $i = 1, \dots, K$: the orientations of the K images.
- Fourier projection-slice theorem

$$R_i \begin{pmatrix} \vec{c}_{ij}^T \\ 0 \end{pmatrix} = R_j \begin{pmatrix} \vec{c}_{ji}^T \\ 0 \end{pmatrix} \text{ for } 1 \leq i < j \leq K.$$

- They are $\binom{K}{2}$ linear equations for the $6K$ variables

Least Squares Approach

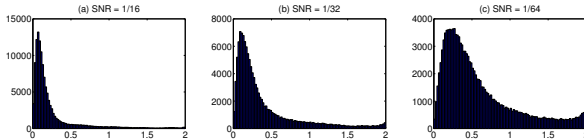
- Weighted LS approach

$$\min_{R_1, \dots, R_K \in \mathbf{SO}(3)} \sum_{i \neq j} w_{ij} \left\| R_i (\vec{c}_{ij}, 0)^T - R_j (\vec{c}_{ji}, 0)^T \right\|^2$$

- Since $\left\| R_i (\vec{c}_{ij}, 0)^T \right\| = \left\| R_j (\vec{c}_{ji}, 0)^T \right\| = 1$, we obtain

$$\max_{R_1, \dots, R_K \in \mathbf{SO}(3)} \sum_{i \neq j} w_{ij} \langle R_i (\vec{c}_{ij}, 0)^T, R_j (\vec{c}_{ji}, 0)^T \rangle$$

- The solution may not be optimal due to the typically large proportion of outliers:



histogram plots of errors: $\left\| R_i (\vec{c}_{ij}, 0)^T - R_j (\vec{c}_{ji}, 0)^T \right\|$

Least Unsquared Deviations

- Sum of unsquared residuals

$$\min_{R_1, \dots, R_K \in \mathbf{SO}(3)} \sum_{i \neq j} \left\| R_i (\vec{c}_{ij}, 0)^T - R_j (\vec{c}_{ji}, 0)^T \right\|^2$$

or

$$\min_{R_1, \dots, R_K \in \mathbf{SO}(3)} \sum_{i \neq j} \left\| (\vec{c}_{ij}, 0)^T - R_i^T R_j (\vec{c}_{ji}, 0)^T \right\|^2$$

- Reweighted Least unsquared problem

$$\min_{R_1, \dots, R_K \in \mathbf{SO}(3)} \sum_{i \neq j} w_{ij} \left\| R_i (\vec{c}_{ij}, 0)^T - R_j (\vec{c}_{ji}, 0)^T \right\|^2$$

- Less sensitive to misidentifications of common-lines (outliers)

Semidefinite Programming Relaxation (SDR)

- Rotations:

$$R_i R_i^T = I_3, \det(R_i) = 1, \text{ for } i = 1, \dots, K$$

- The columns of the rotation matrix R_i :

$$R_i = \begin{pmatrix} | & | & | \\ R_i^1 & R_i^2 & R_i^3 \\ | & | & | \end{pmatrix}, \quad i = 1, \dots, K.$$

- Define a $3 \times 2K$ matrix R :

$$R = \begin{pmatrix} | & | & \cdots & | & | & \cdots & | & | \\ R_1^1 & R_1^2 & \cdots & R_k^1 & R_k^2 & \cdots & R_K^1 & R_K^2 \\ | & | & & | & | & & | & | \end{pmatrix}$$

Semidefinite Programming Relaxation (SDR)

- Objective function:

$$\sum_{i \neq j} w_{ij} \langle R_i (\vec{c}_{ij}, 0)^T, R_j (\vec{c}_{ji}, 0)^T \rangle = \text{trace} ((W \circ S) G)$$

- Gram matrix

$$G = R^T R$$

- G is a rank-3 semidefinite positive matrix

$$G_{ij} = \begin{pmatrix} (R_i^1)^T \\ (R_i^2)^T \end{pmatrix} \begin{pmatrix} R_i^1 & R_i^2 \end{pmatrix}.$$

SDR for weighted LS

- $S = (S_{ij})_{i,j=1,\dots,K}$ and $W = (W_{ij})_{i,j=1,\dots,K}$ are $2K \times 2K$ matrices:

$$S_{ij} = \vec{c}_{ji}^T \vec{c}_{ij}, \text{ and } W_{ij} = w_{ij} \begin{pmatrix} 1 & 1 \\ 1 & 1 \end{pmatrix}.$$

- orthogonality implies

$$G_{ii} = I_2, \quad i = 1, 2, \dots, K$$

- SDR:

$$\begin{aligned} \max_{G \in \mathbb{R}^{2K \times 2K}} \quad & \text{trace} ((W \circ S) G) \\ \text{s.t.} \quad & G_{ii} = I_2, \quad i = 1, 2, \dots, K, \\ & G \succcurlyeq 0 \end{aligned}$$

SDR for LUD

- Define a $3K \times 3K$ matrix $\tilde{G} = (\tilde{G}_{ij})_{i,j=1,\dots,K}$ with $\tilde{G}_{ij} = R_i^T R_j$:

$$\min_{\tilde{G} \succcurlyeq 0} \sum_{i \neq j} \left\| (\vec{c}_{ij}, 0)^T - \tilde{G}_{ij} (\vec{c}_{ji}, 0)^T \right\|, \text{ s.t. } \tilde{G}_{ii} = I_3$$

- If $\{R_i\}$ is a solution, then $\{JR_iJ\}$ is also a solution, where

$$J = \begin{pmatrix} 1 & 0 & 0 \\ 0 & 1 & 0 \\ 0 & 0 & -1 \end{pmatrix}.$$

- Let $\tilde{G}^J = (\tilde{G}_{ij}^J)_{i,j=1,\dots,K}$ with $\tilde{G}_{ij}^J = JR_i^T J J R_j J = JR_i^T R_j J$. Then $\frac{1}{2}(\tilde{G} + \tilde{G}^J)$ is also a solution.

SDR for LUD

- Using the fact that

$$\frac{1}{2}(\tilde{G}_{ij} + \tilde{G}_{ij}^J) = \begin{pmatrix} G_{ij} & 0 \\ 0 & 0 \end{pmatrix},$$

we obtain

$$\min_{G \succcurlyeq 0} \sum_{i \neq j} \|\vec{c}_{ij}^T - G_{ij} \vec{c}_{ji}^T\|, \text{ s.t. } G_{ii} = I_2.$$

- Solved by alternating direction augmented Lagrangian method

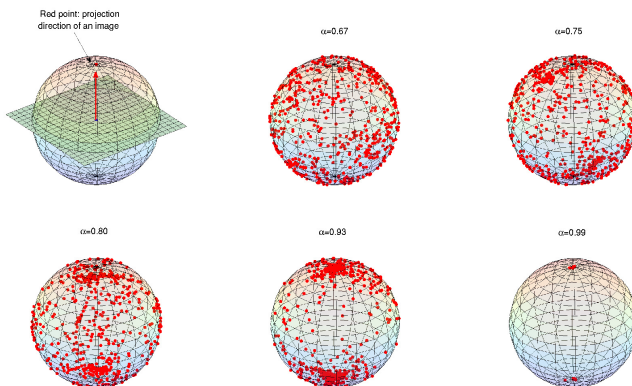
Spectral Norm Constraint

presence of many “outliers” (i.e., a large proportion of misidentified common-lines):

- images whose viewing directions are parallel share many common lines, which is resulted by the overlapping Fourier slices.
- when the viewing directions of R_i and R_j are nearby, the fidelity term $\left\| R_i(\vec{c}_{ij}, 0)^T - R_j(\vec{c}_{ji}, 0)^T \right\|$ can become small, even when the common line pair $(\vec{c}_{ij}, \vec{c}_{ji})$ is misidentified.
- the Gram matrix G has just two dominant eigenvalues, instead of three.

Spectral Norm Constraint

- The dependency of the spectral norm of G (denoted as αK here) on the distribution of orientations of the images. Each red point denotes the viewing direction of a projection. The larger the spectral norm αK is, the more clustered the viewing directions are.



Spectral Norm Constraint

- add constraint on the spectral norm of the Gram matrix G :

$$G \preccurlyeq \alpha K I_{2K}$$

or

$$\|G\|_2 \leq \alpha K$$

- $\alpha \in [\frac{2}{3}, 1)$ controls the spread of the viewing directions
- If true orientations are uniformly sampled $\mathbf{SO}(3)$, then by the law of large numbers and the symmetry of the distribution of orientations, the spectral norm of the true Gram matrix G_{true} is approximately $\frac{2}{3}K$
- If true viewing directions are highly clustered, then the spectral norm of the true Gram matrix G_{true} is close to K .

ADMM for relaxed weighted LS

- Primal problem

$$\begin{aligned} \min_{G \succcurlyeq 0} \quad & -\langle C, G \rangle \\ \text{s.t.} \quad & \mathcal{A}(G) = \mathbf{b} \\ & \|G\|_2 \leq \alpha K \end{aligned}$$

where

$$\mathcal{A}(G) = \begin{pmatrix} G_{ii}^{11} \\ G_{ii}^{22} \\ \frac{\sqrt{2}}{2}G_{ii}^{12} + \frac{\sqrt{2}}{2}G_{ii}^{21} \end{pmatrix}_{i=1,2,\dots,K}, \quad \mathbf{b} = \begin{pmatrix} b_i^1 \\ b_i^2 \\ b_i^3 \end{pmatrix}_{i=1,2,\dots,K},$$

$$b_i^1 = b_i^2 = 1, \quad b_i^3 = 0 \text{ for all } i.$$

ADMM for relaxed weighted LS

- Dual problem

$$\begin{aligned} \min_{\mathbf{y}, X \succcurlyeq 0} \quad & -\mathbf{y}^T \mathbf{b} + \alpha K \|Z\|_* \\ \text{s.t.} \quad & Z = C + X + \mathcal{A}^*(\mathbf{y}) \end{aligned}$$

- ADMM:

$$\mathbf{y}^{k+1} = -\mathcal{A}(C + X^k - Z^k) - \frac{1}{\mu} (\mathcal{A}(G) - \mathbf{b}),$$

$$Z^{k+1} = U \text{diag}(\hat{\mathbf{z}}) U^T, \quad \hat{\mathbf{z}} = \arg \min_{\mathbf{z}} \frac{\alpha K}{\mu} \|\mathbf{z}\|_1 + \frac{1}{2} \|\mathbf{z} - \boldsymbol{\lambda}\|_2^2,$$

$$X^{k+1} = \left(C + X^k + \mathcal{A}^*(\mathbf{y}^{k+1}) + \frac{1}{\mu} G^k \right)_+,$$

$$G^{k+1} = (1 - \gamma) G^k + \gamma \mu (X^{k+1} - H^k).$$

ADMM for relaxed LUD

- Consider the LUD problem

$$\min_{\mathbf{x}_{ij}, G \succcurlyeq 0} \sum_{i < j} \|\mathbf{x}_{ij}\| \text{ s.t. } \mathcal{A}(G) = \mathbf{b}, \mathbf{x}_{ij} = \vec{c}_{ij}^T - G_{ij} \vec{c}_{ji}^T, \|G\|_2 \leq \alpha K$$

- Dual problem

$$\begin{aligned} \min_{\boldsymbol{\theta}_{ij}, \mathbf{y}, X \succcurlyeq 0} \quad & -\mathbf{y}^T \mathbf{b} - \sum_{i < j} \left\langle \boldsymbol{\theta}_{ij}, \vec{c}_{ij}^T \right\rangle + \alpha K \|Z\|_* \\ \text{s.t.} \quad & Z = Q(\boldsymbol{\theta}) + X + \mathcal{A}^*(\mathbf{y}), \quad \text{and } \|\boldsymbol{\theta}_{ij}\| \leq 1. \end{aligned}$$

- Apply ADMM to the dual problem

Iterative Reweighted Least Squares (IRLS)

- SDR:

$$\min_{G \in \mathbb{R}^{2K \times 2K}} F(G) = \sum_{i,j=1,2,\dots,K} \sqrt{2 - 2 \sum_{p,q=1,2} G_{ij}^{pq} S_{ij}^{pq}}$$

$$\text{s.t.} \quad G_{ii} = I_2, \quad i = 1, 2, \dots, K,$$

$$G \succcurlyeq 0,$$

$$\|G\|_2 \leq \alpha K \text{ (optional)}$$

- Smoothing version

$$\min_{G \in \mathbb{R}^{2K \times 2K}} F(G, \epsilon) = \sum_{i,j=1,2,\dots,K} \sqrt{2 - 2 \sum_{p,q=1,2} G_{ij}^{pq} S_{ij}^{pq} + \epsilon^2}$$

$$\text{s.t.} \quad G_{ii} = I_2, \quad i = 1, 2, \dots, K,$$

$$G \succcurlyeq 0,$$

$$\|G\|_2 \leq \alpha K \text{ (optional)}$$

Iterative Reweighted Least Squares (IRLS)

Main steps:

- compute G^{k+1} to be the solution of

$$\min_{G \succcurlyeq 0} \sum_{i \neq j} w_{ij}^k (2 - 2 \langle G_{ij}, S_{ij} \rangle + \epsilon^2) \text{ s.t. } \mathcal{A}(G) = \mathbf{b}, (\|G\|_2 \leq \alpha K)$$

- update

$$w_{ij}^k = 1 / \sqrt{2 - 2 \langle G_{ij}^k, S_{ij} \rangle + \epsilon^2}, \forall k > 0.$$

Convergence:

- the cost function sequence is monotonically non-increasing

$$F(G^{k+1}, \epsilon) \leq F(G^k, \epsilon).$$

- The sequence of iterates $\{G^k\}$ of IRLS is bounded, and every cluster point of the sequence is a stationary point.

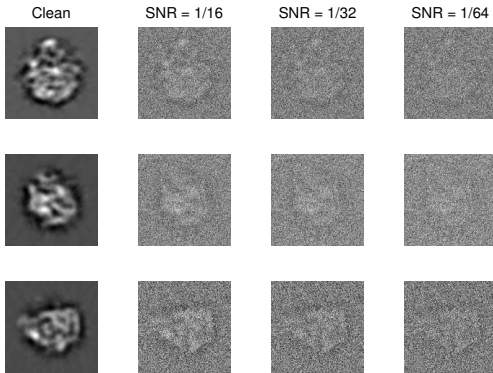
Numerical Results

- 3D Fourier Shell Correlation (FSC). FSC measures the normalized cross-correlation coefficient between two 3D volumes over corresponding spherical shells in Fourier space

$$\text{FSC}(i) = \frac{\sum_{\mathbf{j} \in \text{Shell}_i} \mathcal{F}(\mathbf{V}_1)(\mathbf{j}) \cdot \overline{\mathcal{F}(\mathbf{V}_2)(\mathbf{j})}}{\sqrt{\sum_{\mathbf{j} \in \text{Shell}_i} |\mathcal{F}(\mathbf{V}_1)(\mathbf{j})|^2 \cdot \sum_{\mathbf{j} \in \text{Shell}_i} |\mathcal{F}(\mathbf{V}_2)(\mathbf{j})|^2}}$$

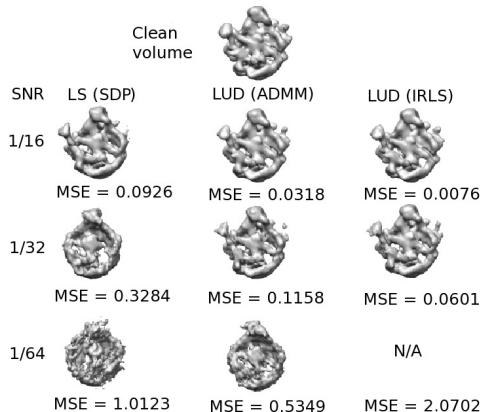
- The reconstruction from the images with estimated orientations used the Fourier based 3D reconstruction package FIRM
- The reconstructed volumes are shown using the visualization system Chimera

Numerical Results: simulated images



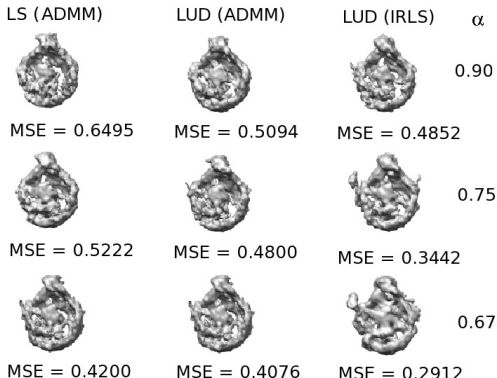
The first column shows three clean images of size 129×129 pixels generated from a 50S ribosomal subunit volume with different orientations. The other three columns show three noisy images corresponding to those in the first column with $\text{SNR} = 1/16, 1/32$ and $1/64$, respectively.

Numerical Results: simulated images



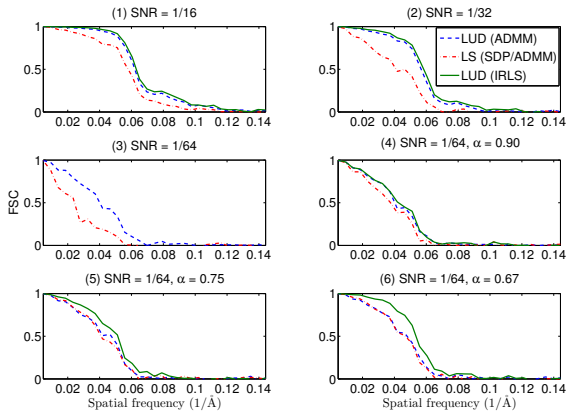
The clean volume (top), the reconstructed volumes and the MSEs. No spectral norm constraint was used (i.e., $\alpha = \text{N/A}$) for all algorithms. The result using the IRLS procedure without α is not available due to the highly clustered estimated projection directions.

Numerical Results: simulated images



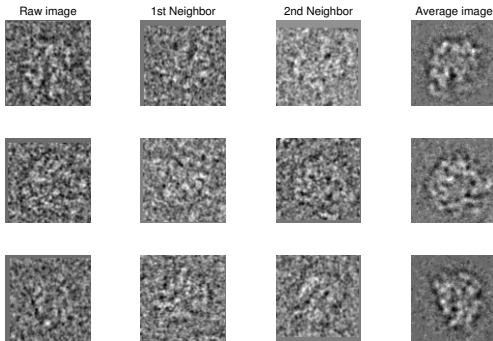
The reconstructed volumes from images with SNR = 1/64 and the MSEs of the estimated rotations using spectral norm constraints (i.e., $\alpha = 0.90, 0.75$, and 0.67) for all algorithms. The result from the IRLS procedure with $\alpha = 0.67$ for the spectral norm constraint is best.

Numerical Results: simulated images



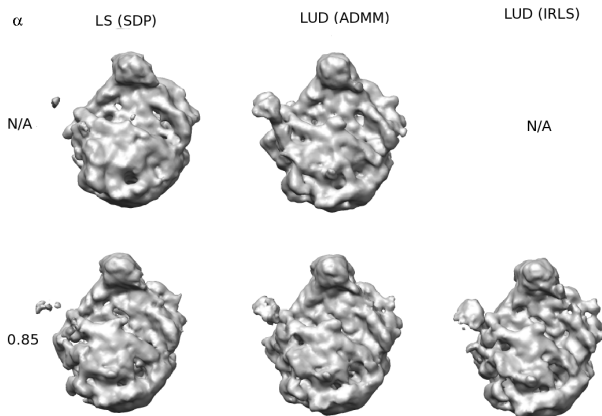
FSCs of the reconstructed volumes against the clean volume

Numerical Results: real dataset



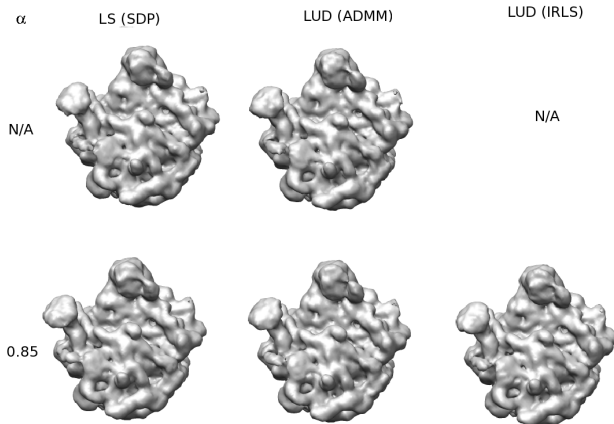
Noise reduction by image averaging. Three raw ribosomal images are shown in the first column. Their closest two neighbours (i.e., raw images having similar orientations after alignments) are shown in the second and third columns. The average images shown in the last column were obtained by averaging over 10 neighbours of each raw image.

Numerical Results: real dataset



The ab-initio models estimated by merging two independent reconstructions, each obtained from 1000 class averages. The resolutions of the models are 17.2 \AA , 16.7 \AA , 16.7 \AA , 16.7 \AA and 16.1 \AA using the FSC 0.143 resolution cutoff.

Numerical Results: real dataset



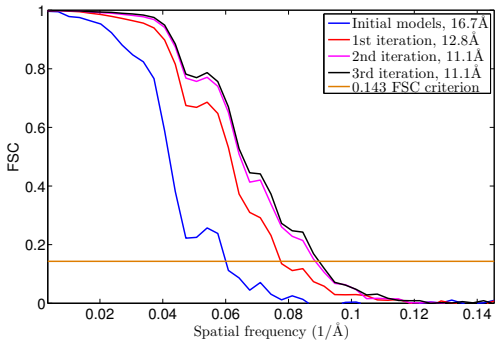
The refined models corresponding to the ab-initio models. The resolutions of the models are all 11.1 Å.

Numerical Results: real dataset

The average cost time using different algorithms on 500 and 1000 images in the two experimental subsections. The notation $\alpha = \text{N/A}$ means no spectral norm constraint $\|G\|_2 \leq \alpha K$ is used.

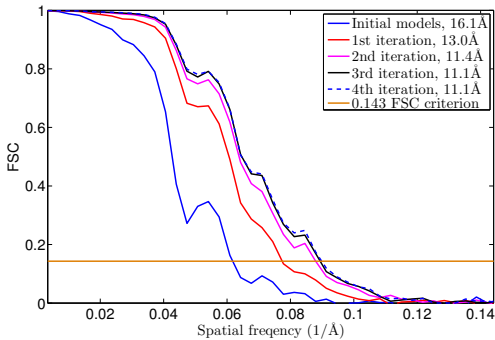
K	$\alpha = \text{N/A}$				$\frac{2}{3} \leq \alpha \leq 1$		
	LS (SDP)	LUD		LS (ADMM)	LUD		ADMM
		ADMM	IRLS		ADMM	IRLS	
500	7s	266s	469s	78s	454s	3353s	
1000	31s	1864s	3913s	619s	1928s	20918s	

Numerical Results: real dataset



LUD, ADMM: Convergence of the refinement process

Numerical Results: real dataset



LUD, IRLS: Convergence of the refinement process